ACS MATERIALS LETTERS

www.acsmaterialsletters.org

A Two-Dimensional Borophene Supercapacitor

Yaser Abdi,* Ali Mazaheri,△ Soheil Hajibaba,△ Sara Darbari, Seyed Javad Rezvani, Andrea Di Cicco, Francesco Paparoni, Reza Rahighi, Somayeh Gholipour, Alimorad Rashidi, Mahdi Malekshahi Byranvand,* and Michael Saliba*

Cite This: *ACS Materials Lett.* 2022, 4, 1929−1936

Read Online

ACCESS | Metrics & More | Article Recommendations | Supporting Information

ABSTRACT: **This work introduces a new two-dimensional (2D) borophene-based (BB) supercapacitor produced by a chemical vapor deposition method and used in the facile fabrication of nanosupercapacitors (spin-coating on graphite substrates). Structural properties of the as-prepared borophene sheets are fully characterized via AFM, HRTEM, and FESEM, and Raman spectrum of the 2D sheets is scrutinized and discussed, as well as the electrochemical response of the fabricated nanosupercapacitors. A high specific capacity (sCap) of 350 F g^{-1} is attributed to the device according to the electrochemical tests, that is almost three times higher than previous boron-based supercapacitors and surpasses the best reported 2D materials including graphene. Based on the surface charge-storage mechanism, it is posited that the electrical conductivity and surface area of 2D electrode materials highly affect the performance of the supercapacitor. Simulation studies are also conducted using joint density-functional theory (JDFT), the results of which are in agreement with the reported outcomes of experiments. Application of the newly synthesized 2D BB supercapacitors in the current study is expected to be promising in the energy storage field, inventive class of sensing devices, as well as novel highly sensitive biosensors.**

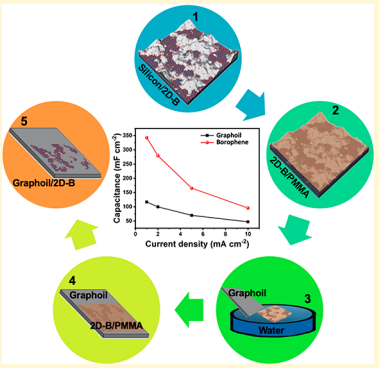

The emergence of supercapacitors can herald next-generation energy storage systems,[1] as their high records of charge storage properties are constantly being reported as of late.[2] Fast charge/discharge cycles of supercapacitors together with their high power densities and long cycling life puts them on a pedestal,[3−5] for their promising usage in energy storage-related devices. They have demonstrated a record power density of 14 W g^{-1} higher than lithium-ion batteries (1.5 W g^{-1}) and capacities of ∼300−3300 F that is greater than the conventional dielectric or electrolytic capacitors (2.7 F).[6−10] Breakthroughs are rationally expected in case exceptional properties of two-dimensional (2D) can be exploited in this booming field of research. For instance, large specific surface area,[11] high physical activity, strong chemical stability, and quantum confinement effects of graphene intrigued their usage in the electric double-layer capacitor (EDLC), owing to its unparalleled conductivity and low large-scale production cost,[12−17] with a highest reported sCap of 200 F g^{-1}.[6,18,19]

Nevertheless, the total sCap of graphene is intrinsically limited due to the quantum capacitance effect,[20] that is caused by its low electronic density of states (DOS) near the Fermi level.[21−23] Doping graphene with boron and nitrogen atoms has been introduced as an approach for tackling this issue by either eliminating the Dirac point or by shifting the Dirac point away from the Fermi level,[20] E.g. sCap of nitrogen-doped thermally expanded graphene oxide could reach to 270 F g^{-1} with discharge current density of 1 A g^{-1}.[20,24,25] However, doping graphene fails to be very much effective and causes immense damage to the crystalline structure of its honeycomb-like lattice.[26] Yet, another way of sCap augmentation would be utilizing alternative 2D materials with better electronic properties and/or higher electronic DOS near the Fermi level.[27]

Recently, borophene is being vastly investigated for possible applications in high-speed electronic devices, flexible and transparent electrodes,[28−31] alkali metal ion batteries,[32−35] hydrogen storage,[36] and superconductors.[37,38] The main synthesis methods of 2D nanosheets have serious limitations, namely CVD, molecular beam epitaxy (MBE), mechanical cleavage, ion intercalation exfoliation, selectively etching, and thermal oxidation etching. Although the top−down prepara-

Received: May 29, 2022
Accepted: August 25, 2022
Published: September 6, 2022

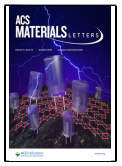

https://doi.org/10.1021/acsmaterialslett.2c00475
ACS Materials Lett. 2022, 4, 1929−1936

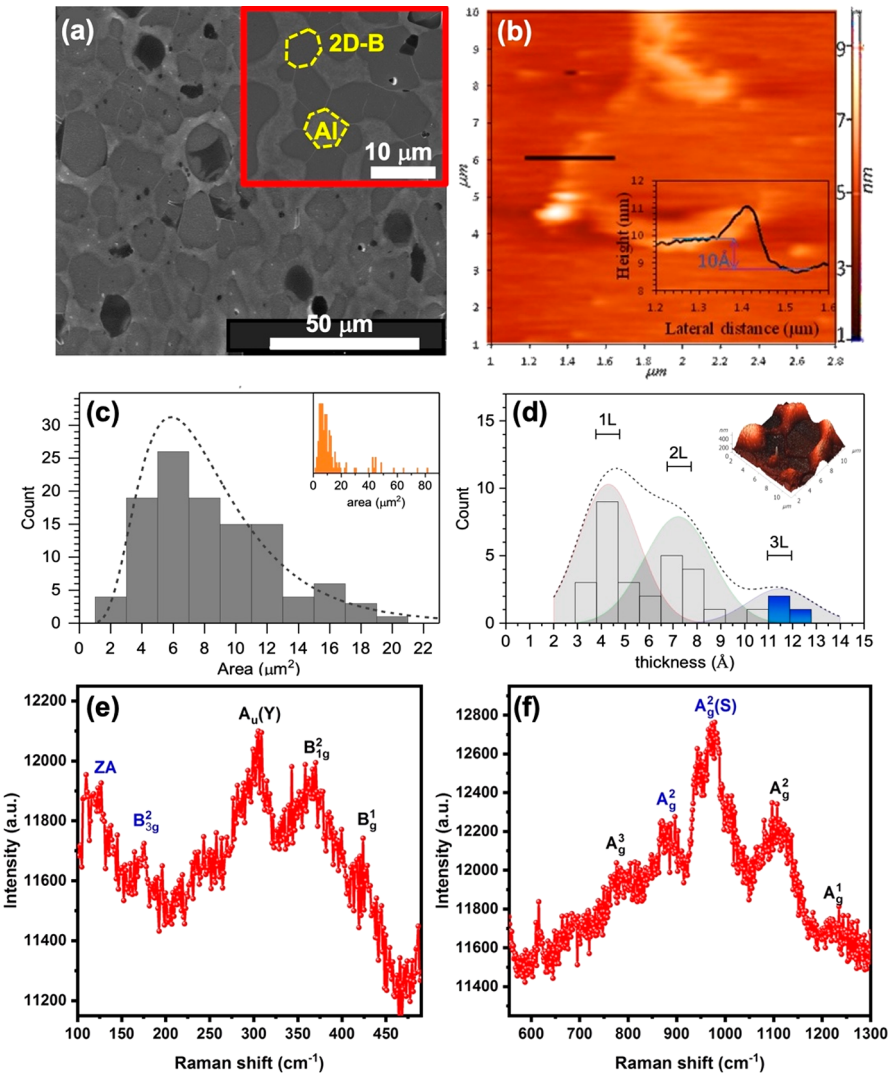

Figure 1. (a) FESEM images of as-prepared borophene sheets on the initial substrate (gray parts, borophenes; bright regions, Al domains). Hexagon-like borophene crystals are separated from the Al aggregated regions via sharp edges as illustrated in the zoomed area (the inset, scale bar corresponds to 10 μm, 2D-B represents 2D borophene). (b) AFM images and size distribution of sheets. (c) Statistical distribution of lateral area of the prepared borophene sheets (inset shows full-scale area distribution). (d) Statistical distribution of thickness of borophene sheets collected over 30 microscale sheets (inset shows an AFM topography image of the as-prepared sample and its corresponding 3D view showing the separation of borophene domains from Al regions). (e and f) Far-field Raman spectrum of χ_3 and β_{12} borophene sheet.

tion method is simpler and more economical, the thickness of resulted borophene is not uniform and the possibility of achieving (single-layer) atomic-thickness is very low. Therefore, developing an efficient method of synthesizing high-quality borophene will help further developments in the area of new BB devices.[39] Synthesis of transferable borophene sheets enables the fabrication of BB nanosupercapacitors.[40] Epitaxial growth of borophene was reported by Wu et al.[41] that needs ultravacuum conditions. Two types of borophene, $\beta_{12,}$ and χ_3 sheets, with the same triangular lattice and different arrangements of hexagonal holes, can be easily formed.[27,41,42] MBE has been used to synthesize borophene on metal substrates with proper crystal lattice matching.[27,41,43−45] The requirement of a single-crystalline metallic substrate restricts the usage of borophene in various electronic devices.

The high cost of Cu(111) limits large-scale borophene fabrication and the small size of the islands hinders delving into its electron transport properties. To avoid the formation of separate islands while synthesizing BB nanostructures, a growth method has been recently proposed[46] for borophene on a copper substrate with the drawback of resulting in thick borophene-like structures. Full coverage of thick Cu(111) films grown on sapphire has been realized; however, via CVD growth of monolayer borophene sheets, having dimensions at the level of micrometers,[47] and crystallization of BB, the structure can be further enhanced by introducing appropriate catalyst in synthesis procedure.[48,49] Substrate-free synthesis of borophene has been scarcely tried, the result of which has been an obstacle for its deep analysis, characterization, scalable production, and possible/potential applications.[50] It is expected that BB heterostructures can have intriguing properties as a result of the unique metallic characteristic of borophene when combined with other 2D materials. Very recently, vertical and lateral heterostructures of borophene with graphene, for instance, were studied functioning as a

https://doi.org/10.1021/acsmaterialslett.2c00475
ACS Materials Lett. 2022, 4, 1929−1936

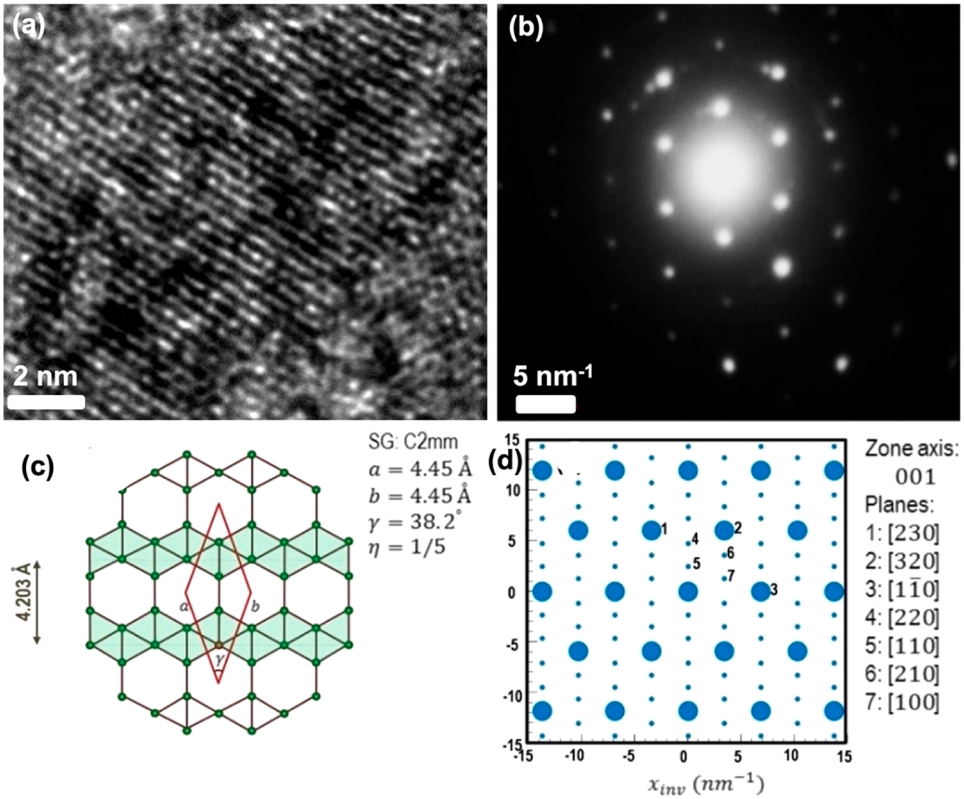

Figure 2. (a) HRTEM lattice image of borophene sheet showing the parallel strips with interdistance of around 4.15 Å, (b) SAED pattern of a typical sheet, (c) lattice structure, and (d) theoretical diffraction pattern of χ_3 the crystal phase of borophene.

metal−semiconductor junction,[51] results of which highlighted the potential of creating novel integrated nanocircuits.

Herein, a low-cost and scalable chemical vapor deposition (CVD) approach is developed to synthesize high-quality and transferable borophene sheets to the desired substrates. As a result, highly efficient nanosupercapacitors are fabricated by depositing borophene sheets on graphite substrates, leading to an excellent sCap of 350 F g^{-1} for 2D supercapacitors. Moreover, a simulation study to support the experimental findings is performed. This approach creates the possibility of a breakthrough in the field of energy storage and supercapacitors based on borophene sheets.

The growth of borophene sheets was conducted using Al-assisted CVD on Si wafer substrate[52] (as summarily illustrated in Figure S1). The synthesized borophene sheets were initially subject to a complete morphological and structural analysis. Figure 1a provides results of field emission scanning electron microscope (FESEM) investigations as the morphological and topographical characteristics of the synthesized borophene sheets. The gray parts (nanosheets of borophene) and the bright zones (Al islands) on the silicon substrate can be distinguished in the inset of Figure 1a. The polygon shape of the borophene domains, which are separated from Al islands by nearly sharp edges, depicts the long-range order crystalline structure of the synthesized sheets. More images of transferred sheets are presented in Figures S2−S4. The thickness of the transferred borophene sheets is measured to be a few angstroms, as seen in Figures 1b and S5b. According to AFM images, the sheets present a statistical distribution with a mean area of around 6 μm^2, while wider borophene sheets with a lateral area of 40−50 μm^2 exist in all samples (inset of Figure 1c). The overall thickness distribution also reveals a meaningful partitioning of the measured heights into three subdivisions (see Figure 1d). A partial edge peel-up of the transferred borophene sheets (see Figure S3B) leads to a height increment at the sheet edges in the height profile of the inset of Figure 1b.

Kernel distribution of Figure 1d can be finely fitted by three Gaussian distributions centered at 4.2 Å, 7.4 Å, and 11.5 Å that can be assigned to mono-, bi-, and trilayer borophene, respectively. The thickness of the borophene sheet on the clean metal substrate has been reported to be around 3.0 Å.[41,43] Raman fingerprints of borophene suggest the coexistence of primarily χ3 phases (components at 300, 375, 430, 780, 1100, and 1240 cm^{-1}) along with some signature of the β12 phase (components at 125, 175, 900, and 980 cm^{-1}) of borophene (see Figure 1e and f).[53] Since the boron and borophene are deposited on the Si substrate, the main Raman peak of silicone is located at 520 cm^{-1} (see Figure S6). In contrast to graphene, borophene is anisotropic without identical symmetry axes, leading to the split of the scattering modes. Moreover, regardless of graphene, other parameters such as defects and atomic displacements toward atomic ridges would contribute extra Raman peaks.[42]

Bright-field TEM analysis of two synthesized borophene sheets along with the selected area electron diffraction (SAED) also confirmed the presence of the χ_3 phase of the borophene sheet (see Figure 2a, b, and Figure S4a). The HRTEM image of a borophene sheet clearly demonstrates the parallel atomic strips with an average distance of about 4.15 Å, which is in perfect agreement with the distance between parallel strip-like regions of high atomic concentration in χ_3-sheet (4.20 Å). Comparing Figure 2b and d shows a good agreement between the observed diffraction pattern and the primary reciprocal

https://doi.org/10.1021/acsmaterialslett.2c00475
ACS Materials Lett. 2022, 4, 1929−1936

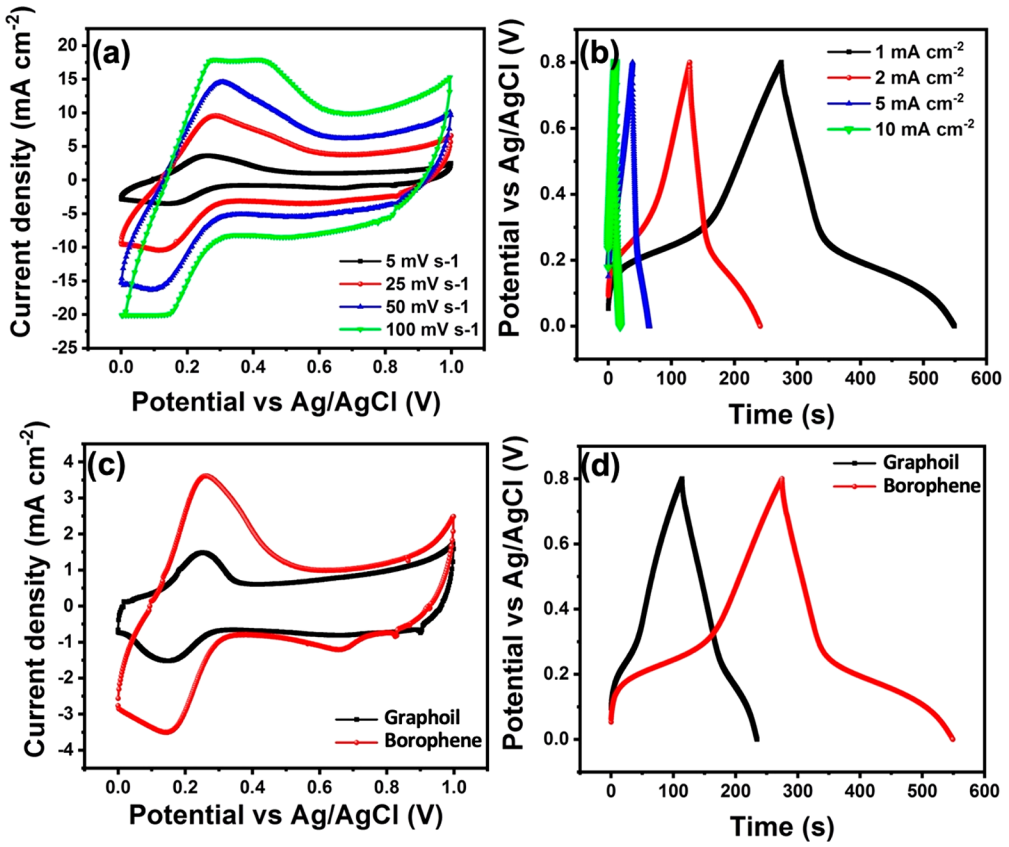

Figure 3. Electrochemical analysis of the supercapacitor. (a) Cyclic voltammograms at different scan rates (b) Galvanostatic charge/discharge test at different current densities. (c, d) A comparison between the electrochemical performance of the supercapacitors based on the pristine graphoil and the borophene-coated one.

lattice of borophene sheets,[52] that is, larger spots. The size of each disk in Figure 2d is calculated according to the structure factor of the atomic lattice, which is directly proportional to the intensity of the diffracted beam.

Electrochemical properties of 2D borophene are found to be better in comparison with graphene as the results show, thus being a more suitable electrode material[54] in applications like batteries[55] and supercapacitors. These properties are described as follows: (I) large and stable voltage window, (II) suitable sCap, (III) excellent rate capability, (IV) good cycling stability, and (V) excellent energy density. Supercapacitive properties of the borophene sheets were investigated by depositing the sheets on the graphoil by a wet-transfer method. A thin layer of the hydrophobic polymer was deposited on the borophene/silicon wafer to assist the borophene soaking in the distilled water surface. The fabrication process of the BB supercapacitors is reported in the Experimental Section and schematically shown in Figures S1a and S3. Electrochemical analysis of the prepared nanosupercapacitors with borophene/graphoil working electrode was carried out by cyclic voltammetry in the potential range of 0 to 1 V at different scan rates. The electrochemical behavior of borophene for supercapacitors was first investigated in 1 M sulfuric acid in a three electrodes configuration, in which the borophene coated graphoil was used as working electrodes, and a platinum bar and a saturated Ag/AgCl were employed as counter and reference electrodes. To compare the performance of the supercapacitor device, a two-electrode system was also analyzed (see Figure S7). Figures 3 and 4 show the results of electrochemical analyses of the fabricated supercapacitors. Cyclic voltammograms (CVs) at different scan rates are presented in Figure 3a. The analogous shape of the CV plot in the three BB electrodes possesses redox anodic and cathodic peaks, which result from pseudocapacitance. However, a double-layer capacitance gives a CV curve close to an ideal rectangular shape.[56,57]

The CV curves measured from 5 to 100 mV s^{-1} indicate a good capacitive behavior (from 275 to 110 mF cm^{-2}). A galvanostatic charge/discharge (GCD) test at different current densities was also conducted to calculate the sCap (see and the results are shown in Figure 3b). The higher sCap of the borophene sheets is clearly visible in comparison with an uncoated graphoil electrode by an increase of the $J-V$ area curve (see Figure 3a). A comparison between the electrochemical performance of the supercapacitors based on the pristine graphoil and the borophene-coated one is provided in Figures 3c and 3d. As can be seen, the area of the $J-V$ curve of the control sample (graphoil) has increased (from 1.25 to 3.5 cm^2) significantly after borophene coating, which implies the higher sCap.

Figure 3d depicts the $V-T$ curves at 1 A g^{-1} current density, evidence of doubled discharge times for borophene supercapacitor, compared with the reference (graphoil) electrode. Our analysis, based on the area-normalized and sCap demonstrated a capacitance as high as 0.75 F g^{-1} (350 mF cm^{-2}) for borophene coated electrodes. Moreover, it can be seen in Figure 4b that the capacitance reached around 0.58 F g^{-1} (270 mF cm^{-2}), at the scan rate of 5 mV s^{-1}, and decreased accordingly by increasing the scan rate. The results show that at 1 mA cm^{-2} current density, the sCap of graphoil increases

https://doi.org/10.1021/acsmaterialslett.2c00475
ACS Materials Lett. 2022, 4, 1929−1936

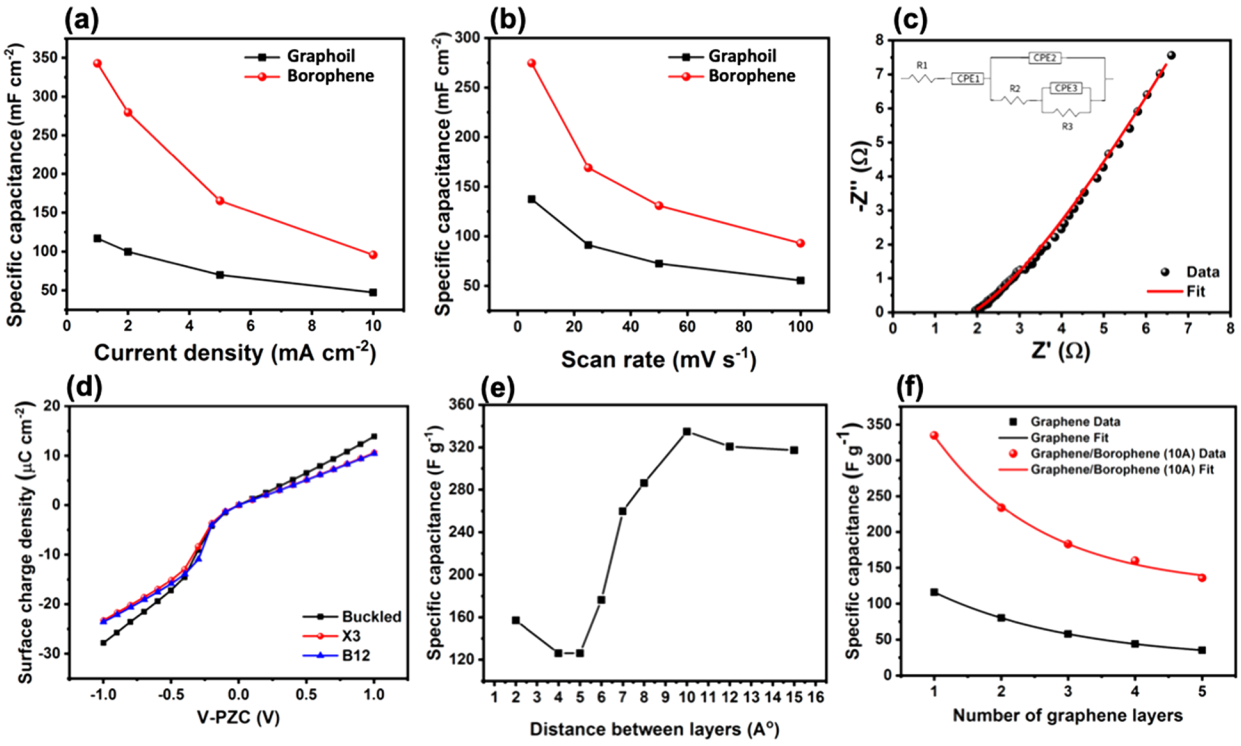

Figure 4. Electrochemical analysis of the supercapacitor. Area-normalized and sCap calculated from GCD test (a) and CV measurement (b). (c) Nyquist plot of the BB supercapacitor (inset: equivalent circuit describing the Nyquist plot). Simulation results of (d) surface charge density versus the applied voltage, (e) the sCap of bilayer borophene/graphene with different interlayer distances, and (f) the sCap of graphene and borophene/graphene versus the number of graphene layers.

from 0.25 (117 mF cm^{-2}) to 0.75 F g^{-1}. The weight of the pristine graphoil in this study was 710 mg. Accordingly, a 0.35 F increment was achieved by coating the borophene sheets on graphoil. The weight of added borophene sheets on graphoil in this study was always less than 1 mg for different experiments. Thus, the sCap of the pure borophene sheets is higher than 350 F g^{-1}. Moreover, to study the mere capacitance of the device, a two-electrode system was fabricated, the sCap of which was tested to be 30% lower than that of the three-electrode system. It is worth mentioning that in the three-electrode configuration, the capacitance of the electrode materials is involved as well (arising from the geometrical area of the substrate, accessible electrolyte, and mass deposition). After the performed electrochemical analysis, unfortunately, the morphology of the atomic-thin borophene could not be easily detectable from the SEM analysis as the stability of the 2D borophene sample may be susceptible to exposure to ambient oxygen.

The interfacial recombination and transport mechanism in electrodes were investigated using electrochemical impedance spectroscopy (EIS) at a 10 mV AC signal and 100 kHz to 10 MHz frequency range. The Nyquist plot of the BB supercapacitor is shown in Figure 4c. The intersection point with the *x*-axis (in the high-frequency region of EIS plots) indicates the equivalent series resistance (R_s), which mainly arises from the contact resistance of the electrolyte/electrode surface, resistance, the intrinsic resistances of the active material, substrate and electrolyte. The diameter of the semicircle (in the EIS plots) corresponds to the charge-transfer resistance (R_{ct}). Therefore, after the introduction of borophene, the electrical conductivity is increased and charge transfer ability accelerated within the electrodes, as a result of the reduction in both R_s and R_{ct}, as can be seen in Figure 4c,[58,59] Using the fitted curve and the equivalent circuit (see inset of Figure 4c), the attributed parameters of the supercapacitor can be obtained as listed in Table S3. The equivalent circuit contains a series resistance (R1), charge transfer resistances (R2, and R3), and a constant phase element (CPE). The later element is an imperfect capacitor, which stems from the interface capacitor (CPE-T (P1, P2, P3)) and the ideal capacitor (CPE-P (n1, n2, n3)).

Joint density-functional theory (JDFT) was used in our investigation to calculate the sCap of the self-standing borophene sheets and stacked borophene on graphoil (see the Experimental Section for the details). The calculated structures are presented in Figure S8 with the top views of the β_{12} relaxed structures (Figure S8a), striped (Figure S8b), and χ_3 (Figure S8c) phases of the borophene and side view of borophene/graphene stacked layers (Figure S8d). To obtain a stable crystal structure, optimization of the primary cell was done by atomic force relaxation for the relaxation threshold of 0.001 eV $Å^{-1}$.

The DOSs calculation of the self-standing borophene (Figure S9a−c) clearly shows metallic behavior. The relative energies (ΔE), and potential at the point of zero charges (V_{PZC}) referenced to the standard hydrogen electrode (SHE) for the three phases of borophene (see Figure 4d) were also obtained (see Table 1). By integrating the surface charge over the voltage window the area-normalized and mass-normalized capacitances of the three phases of borophene were achieved and provided in Table 1. As expected from our experimental investigation, the capacitances of the borophene phases resulted to be 4−7 times higher than that of the other 2D materials comparison between the calculated capacitances

https://doi.org/10.1021/acsmaterialslett.2c00475
ACS Materials Lett. 2022, 4, 1929−1936

Table 1. Relative Energies (ΔE), the Potential at the Point of Zero Charges (PZC), Real Capacitance, and sCap of Three Phases of Borophene

borophene phase	ΔE (meV atom^{-1})	VPZC vs SHE (V)	areal capacitance (F cm^{-2})	SCap (F g^{-1})
striped	5.67	0.27	19.8	467.9
β_{12}	6.24	0.10	18.3	600.3
χ_3	6.25	−0.02	16.9	576.2

(468−600 F g^{-1}) and the experimentally obtained capacitance for the borophene sheets (higher than 350 F g^{-1}) shows a good agreement between the experiment and simulation.

To consider the graphoil effect as substrate in our experiment, the calculations were performed on the capacitance of the configuration of the stacked layers as shown in Figure S8d. Initially, a bilayer borophene/graphene was considered in the calculation for which the only stable geometry relaxation was found to be striped borophene/graphene with a relative spacing of about 2 Å. Considering that no atomic interaction occurs between staked synthesized borophene and graphoil, the calculation of the sCap of the bilayer borophene/graphene with different distances was performed. Our analysis shows that by increasing the interlayer distance the sCap increases, and it reaches its maximum value for the distances upper than 10 Å (see Figure 4e). The simulation with a distance value of 10 Å perfectly matches our fabricated borophene/graphoil stacked structure. The number of graphene layers increased in a subsequent step to simulate the graphoil substrate (i.e., many layers of graphene or graphite structure). As the number of graphene layers increases, the areal capacitance increases as well, however since the specific area decreases with the number of layers, the sCap decreases proportionally (as simulated in Figure S10). Figure 4f shows the calculated capacitance versus the number of layers for graphene and borophene/graphene. A more realistic value can be achieved by extrapolating the curves to infinite numbers of graphene (here, we considered just five layers of graphene). Our calculation also indicates a capacitance of the borophene/graphene that is almost three times higher than that of graphene layers, which is in good agreement with our electrochemical measurement. Moreover, as shown in Figure 4d, the surface charge density of χ_3 phase is on par with that of β_{12}, which is lower than that of Buckled phase.

Borophene sheets were successfully grown using a simple CVD approach. According to the structural analysis, it was confirmed that χ_3 phase is the dominant structure obtained in this approach. The JDFT simulations showed that this phase is one of the best options for the fabrication of supercapacitors. Due to the ability to transfer synthesized borophene sheets on any desired substrates, we were able to fabricate the highly efficient BB supercapacitors in this work for the first time. To investigate the electrochemical behavior of the borophene sheets, we used graphoil as substrates. Experimental results show that coating the borophene sheets increased the graphoil capacitance up to 0.75 F g^{-1} (350 mF cm^{-2}) which is regarded as a highly efficient device for such substrate. This capacitance was achieved by adding borophene sheets of less than 1 mg. An increment in the capacitance of the pristine graphoil by coating the borophene sheets means that the sCap of the borophene sheets is higher than 350 F g^{-1}, which was confirmed by our simulation results. Such capacitance is three times higher than the reported capacitance for the best reported BB supercapacitors. The results of this work will open up a new window for the fabrication of supercapacitors by utilizing the borophene sheets transferred on different substrates such as activated carbon and nanostructured porous materials to achieve higher capacitances.

4. EXPERIMENTAL SECTION

Synthesis of Borophene. Growth of borophene was conducted by an Al-assisted CVD approach, where a 100 nm thickness of Al was deposited on the growth substrate (the (100) p-type Si wafer), which was initially cleaned by RCA#1 solution. Therefore, the homemade quartz CVD chamber of the deposition system was vacuumed up to the pressure of 3×10^{-3} Torr and then the temperature was ramped up to 830 K in 15 min and the Al-coated substrate was annealed for 1 h with 20 sccm continuous H_2 flow. Subsequently, a gas mixture of 15 sccm B_2H_6 (diborane) and 40 sccm H_2 was introduced into the quartz chamber. After 10 min, the flow of Diborane was interrupted and the furnace is cold down in 3 h to room temperature in an H_2 ambient atmosphere. In this process, the borophene sheets were synthesized on the Al-coated substrate. Schematic of the CVD system and the parameter controlling during the growth step are provided in Figure S1b.

■ ASSOCIATED CONTENT

Supporting Information

The Supporting Information is available free of charge at https://pubs.acs.org/doi/10.1021/acsmaterialslett.2c00475.

CVD growth of borophene, FESEM images, schematics of BB supercapacitors, AFM and TEM images, and Raman spectra of borophene sheets and details of electrode preparation, electrical measurements, and simulation implementation (PDF)

■ AUTHOR INFORMATION

Corresponding Authors

Yaser Abdi − *Nanophysics Research Laboratory, Department of Physics, University of Tehran, Tehran 14395-547, Iran;* orcid.org/0000-0002-7583-7687; Email: y.abdi@ut.ac.ir

Mahdi Malekshahi Byranvand − *Institute for Photovoltaics (ipv), University of Stuttgart, Stuttgart D-70569, Germany; Helmholtz Young Investigator Group FRONTRUNNER, IEK5-Photoevoltaik, Forschungszentrum, Jülich 52425, Germany*; Email: mahdi.malekshahi@ipv.uni-stuttgart.de

Michael Saliba − *Institute for Photovoltaics (ipv), University of Stuttgart, Stuttgart D-70569, Germany; Helmholtz Young Investigator Group FRONTRUNNER, IEK5-Photoevoltaik, Forschungszentrum, Jülich 52425, Germany;* orcid.org/0000-0002-6818-9781; Email: michael.saliba@ipv.uni-stuttgart.de

Authors

Ali Mazaheri − *Nanophysics Research Laboratory, Department of Physics, University of Tehran, Tehran 14395-547, Iran*

Soheil Hajibaba − *Nanophysics Research Laboratory, Department of Physics, University of Tehran, Tehran 14395-547, Iran;* orcid.org/0000-0003-2040-0995

Sara Darbari − *Nano-Sensors and Detectors Laboratory, and Nano-Plasmophotonic Research Group, Faculty of Electrical and Computer Engineering, Tarbiat Modares University, Tehran 14115-194, Iran*

https://doi.org/10.1021/acsmaterialslett.2c00475
ACS Materials Lett. 2022, 4, 1929−1936

Seyed Javad Rezvani − *Physics Division, School of Science and Technology, Università di Camerino Via Madonna delle Carceri 9, 62032 Camerino, Italy;* orcid.org/0000-0002-6771-170X

Andrea Di Cicco − *Physics Division, School of Science and Technology, Università di Camerino Via Madonna delle Carceri 9, 62032 Camerino, Italy*

Francesco Paparoni − *Physics Division, School of Science and Technology, Università di Camerino Via Madonna delle Carceri 9, 62032 Camerino, Italy;* orcid.org/0000-0002-8210-7586

Reza Rahighi − *SKKU Advanced Institute of Nano-Technology (SAINT), Sungkyunkwan University, Suwon, Gyeonggi-do 16419, Republic of Korea*

Somayeh Gholipour − *Nanophysics Research Laboratory, Department of Physics, University of Tehran, Tehran 14395-547, Iran; METU GUNAM Center, Middle East Technical University, Ankara 06800, Turkey;* orcid.org/0000-0001-8935-4515

Alimorad Rashidi − *Nanotechnology Research Center, Research Institute of Petroleum Industry (RIPI), 14857-33111 Tehran, Iran;* orcid.org/0000-0001-6753-1939

Complete contact information is available at: https://pubs.acs.org/10.1021/acsmaterialslett.2c00475

Author Contributions

△A.M. and S.H. contributed equally to this work. Y.A: Conceptualization and design of the method, generating original draft and supervision; A.M: Conducting the experiments (borophene synthesis); S.H: Supercapacitor measurements and implementation of simulations; S.D: Structural analysis and reviewing; S.J.R, A.D.C, and F.P: Analyzing AFM and Raman data; R.R: Creating tables, writing and reviewing; S.G: Literature review, writing and creating figures; A.R. and M.M.B: Reviewing & editing; M.S: Revising & supervision. All authors have given approval to the final version of the manuscript.

Notes

The authors declare no competing financial interest.

■ ACKNOWLEDGMENTS

Y.A. acknowledges the Iran National Science Foundation. M.S. thanks the German Research Foundation (DFG) for funding (SPP2196, 431314977/GRK 2642). M.S. acknowledges funding by ProperPhotoMile. Project ProperPhotoMile is supported under the umbrella of SOLAR-ERA.NET Cofund 2 by the Spanish Ministry of Science and Education and the AEI under the project PCI2020-112185 and CDTI project number IDI-20210171; the Federal Ministry for Economic Affairs and Energy on the basis of a decision by the German Bundestag project number FKZ 03EE1070B and FKZ 03EE1070A. SOLAR-ERA.NET is supported by the European Commission within the EU Framework Programme for Research and Innovation HORIZON 2020 (Cofund ERA-NET Action, No. 786483).

■ REFERENCES

(1) Liu, S.; Kang, L.; Henzie, J.; Zhang, J.; Ha, J.; Amin, M. A.; Hossain, M. S. A.; Jun, S. C.; Yamauchi, Y. Recent Advances and Perspectives of Battery-Type Anode Materials for Potassium Ion Storage. *ACS Nano* **2021**, *15*, 18931−18973.

(2) Liu, S.; Kang, L.; Hu, J.; Jung, E.; Zhang, J.; Jun, S. C.; Yamauchi, Y. Unlocking the Potential of Oxygen-Deficient Copper-Doped Co3O4 Nanocrystals Confined in Carbon as an Advanced Electrode for Flexible Solid-State Supercapacitors. *ACS Energy Lett.* **2021**, *6*, 3011−3019.

(3) Simon, P.; Gogotsi, Y. Materials for Electrochemical Capacitors. *Nat. Mater.* **2008**, *7*, 845−854.

(4) Yan, J.; Wang, Q.; Wei, T.; Fan, Z. Recent Advances in Design and Fabrication of Electrochemical Supercapacitors with High Energy Densities. *Adv. Energy Mater.* **2014**, *4*, 1300816.

(5) Liu, C.; Li, F.; Ma, L.-P.; Cheng, H.-M. Advanced Materials for Energy Storage. *Adv. Mater.* **2010**, *22*, E28−E62.

(6) Zhang, L. L.; Zhao, X. S. Carbon-Based Materials as Supercapacitor Electrodes. *Chem. Soc. Rev.* **2009**, *38*, 2520−2531.

(7) Wang, J.; Polleux, J.; Lim, J.; Dunn, B. Pseudocapacitive Contributions to Electrochemical Energy Storage in TiO2 (Anatase) Nanoparticles. *J. Phys. Chem. C* **2007**, *111*, 14925−14931.

(8) Sassin, M. B.; Chervin, C. N.; Rolison, D. R.; Long, J. W. Redox Deposition of Nanoscale Metal Oxides on Carbon for Next-Generation Electrochemical Capacitors. *Acc. Chem. Res.* **2013**, *46*, 1062−1074.

(9) Sarangapani, S.; Tilak, B. V.; Chen, C.-P. Materials for Electrochemical Capacitors: Theoretical and Experimental Constraints. *J. Electrochem. Soc.* **1996**, *143*, 3791.

(10) Makino, S.; Ban, T.; Sugimoto, W. Towards Implantable Bio-Supercapacitors: Pseudocapacitance of Ruthenium Oxide Nanoparticles and Nanosheets in Acids, Buffered Solutions, and Bioelectrolytes. *J. Electrochem. Soc.* **2015**, *162*, A5001.

(11) Bolhasani, E.; Razi Astaraei, F.; Honarpazhouh, Y.; Rahighi, R.; Yousefzadeh, S.; Panahi, M.; Orooji, Y. Delving into Role of Palladium Nanoparticles-Decorated Graphene Oxide Sheets on Photoelectrochemical Enhancement of Porous Silicon. *Inorg. Chem. Commun.* **2022**, *135*, 109081.

(12) Mahmoudian, L.; Rashidi, A.; Dehghani, H.; Rahighi, R. Single-Step Scalable Synthesis of Three-Dimensional Highly Porous Graphene with Favorable Methane Adsorption. *Chem. Eng. J.* **2016**, *304*, 784−792.

(13) Mostazo-López, M. J.; Ruiz-Rosas, R.; Morallón, E.; Cazorla-Amorós, D. Nitrogen Doped Superporous Carbon Prepared by a Mild Method. Enhancement of Supercapacitor Performance. *Int. J. Hydrogen Energy* **2016**, *41*, 19691−19701.

(14) Wang, T.; Le, Q.; Zhang, G.; Zhu, S.; Guan, B.; Zhang, J.; Xing, S.; Zhang, Y. Facile Preparation and Sulfidation Analysis for Activated Multiporous Carbon@NiCo2S4 Nanostructure with Enhanced Supercapacitive Properties. *Electrochim. Acta* **2016**, *211*, 627−635.

(15) Ahmed, S.; Bhat, Y.; Rafat, M.; Hashmi, S. A. Low-Temperature Thermal Exfoliation of Graphene Oxide for High Performance Supercapacitor. *Journal of Materials Science and Surface Engineering* **2017**, *5*, 571−576.

(16) Geng, P.; Zheng, S.; Tang, H.; Zhu, R.; Zhang, L.; Cao, S.; Xue, H.; Pang, H. Transition Metal Sulfides Based on Graphene for Electrochemical Energy Storage. *Adv. Energy Mater.* **2018**, *8*, 1703259.

(17) Rahighi, R.; Akhavan, O.; Zeraati, A. S.; Sattari-Esfahlan, S. M. All-Carbon Negative Differential Resistance Nanodevice Using a Single Flake of Nanoporous Graphene. *ACS Appl. Electron. Mater.* **2021**, *3*, 3418−3427.

(18) Stoller, M. D.; Park, S.; Zhu, Y.; An, J.; Ruoff, R. S. Graphene-Based Ultracapacitors. *Nano Lett.* **2008**, *8*, 3498−3502.

(19) Chen, Y.; Zhang, X.; Zhang, D.; Yu, P.; Ma, Y. High Performance Supercapacitors Based on Reduced Graphene Oxide in Aqueous and Ionic Liquid Electrolytes. *Carbon* **2011**, *49*, 573−580.

(20) Vatamanu, J.; Ni, X.; Liu, F.; Bedrov, D. Tailoring Graphene-Based Electrodes from Semiconducting to Metallic to Increase the Energy Density in Supercapacitors. *Nanotechnology* **2015**, *26*, 464001.

(21) Zhan, C.; Neal, J.; Wu, J.; Jiang, D. Quantum Effects on the Capacitance of Graphene-Based Electrodes. *J. Phys. Chem. C* **2015**, *119*, 22297−22303.

(22) Brooksby, P.; Farquhar, A. K.; Dykstra, H. M.; Waterland, M.; Downard, A. Quantum Capacitance of Aryldiazonium Modified Large Area Few-Layer Graphene Electrodes. *J. Phys. Chem. C* **2015**, *119*, 25778−25785.

(23) Shan, X.; Chen, S.; Wang, H.; Chen, Z.; Guan, Y.; Wang, Y.; Wang, S.; Chen, H.-Y.; Tao, N. Mapping Local Quantum Capacitance and Charged Impurities in Graphene via Plasmonic Impedance Imaging. *Adv. Mater.* **2015**, *27*, 6213−6219.
(24) Zou, Y.; Kinloch, I. A.; Dryfe, R. A. W. Nitrogen-Doped and Crumpled Graphene Sheets with Improved Supercapacitance. *J. Mater. Chem. A* **2014**, *2*, 19495−19499.
(25) Wang, K.; Li, L.; Zhang, T.; Liu, Z. Nitrogen-Doped Graphene for Supercapacitor with Long-Term Electrochemical Stability. *Energy* **2014**, *70*, 612−617.
(26) Araujo, P. T.; Terrones, M.; Dresselhaus, M. S. Defects and Impurities in Graphene-like Materials. *Mater. Today* **2012**, *15*, 98−109.
(27) Feng, B.; Zhang, J.; Zhong, Q.; Li, W.; Li, S.; Li, H.; Cheng, P.; Meng, S.; Chen, L.; Wu, K. Experimental Realization of Two-Dimensional Boron Sheets. *Nature Chem.* **2016**, *8*, 563−568.
(28) Zhang, Z.; Penev, E. S.; Yakobson, B. I. Polyphony in B Flat. *Nature Chem.* **2016**, *8*, 525−527.
(29) Penev, E. S.; Bhowmick, S.; Sadrzadeh, A.; Yakobson, B. I. Polymorphism of Two-Dimensional Boron. *Nano Lett.* **2012**, *12*, 2441−2445.
(30) Wu, X.; Dai, J.; Zhao, Y.; Zhuo, Z.; Yang, J.; Zeng, X. C. Two-Dimensional Boron Monolayer Sheets. *ACS Nano* **2012**, *6*, 7443−7453.
(31) Zhang, Z.; Yang, Y.; Penev, E. S.; Yakobson, B. I. Elasticity, Flexibility, and Ideal Strength of Borophenes. *Adv. Funct. Mater.* **2017**, *27*, 1605059.
(32) Zhang, Y.; Sun, L.; Bai, L.; Si, H.; Zhang, Y.; Zhang, Y. N-Doped-Carbon Coated Ni2P-Ni Sheets Anchored on Graphene with Superior Energy Storage Behavior. *Nano Res.* **2019**, *12*, 607−618.
(33) Zhang, X.; Hu, J.; Cheng, Y.; Yang, H. Y.; Yao, Y.; Yang, S. A. Borophene as an Extremely High Capacity Electrode Material for Li-Ion and Na-Ion Batteries. *Nanoscale* **2016**, *8*, 15340−15347.
(34) Jiang, H. R.; Lu, Z.; Wu, M. C.; Ciucci, F.; Zhao, T. S. Borophene: A Promising Anode Material Offering High Specific Capacity and High Rate Capability for Lithium-Ion Batteries. *Nano Energy* **2016**, *23*, 97−104.
(35) Yi, T.; Zheng, B.; Yu, H.; Xie, Y. Structures, Stabilities and Work Functions of Alkali-Metal-Adsorbed Boron A1-Sheets. *Chem. Res. Chin. Univ.* **2017**, *33*, 631−637.
(36) Zhang, F.; Chen, R.; Zhang, W.; Zhang, W. A Ti-Decorated Boron Monolayer: A Promising Material for Hydrogen Storage. *RSC Adv.* **2016**, *6*, 12925−12931.
(37) Penev, E. S.; Kutana, A.; Yakobson, B. I. Can Two-Dimensional Boron Superconduct? *Nano Lett.* **2016**, *16*, 2522−2526.
(38) Zhao, Y.; Zeng, S.; Ni, J. Superconductivity in Two-Dimensional Boron Allotropes. *Phys. Rev. B* **2016**, *93*, 014502.
(39) Ou, M.; Wang, X.; Yu, L.; Liu, C.; Tao, W.; Ji, X.; Mei, L. The Emergence and Evolution of Borophene. *Advanced Science* **2021**, *8*, 2001801.
(40) Chand, H.; Kumar, A.; Krishnan, V. Borophene and Boron-Based Nanosheets: Recent Advances in Synthesis Strategies and Applications in the Field of Environment and Energy. *Advanced Materials Interfaces* **2021**, *8*, 2100045.
(41) Wu, R.; Drozdov, I. K.; Eltinge, S.; Zahl, P.; Ismail-Beigi, S.; Božović, I.; Gozar, A. Large-Area Single-Crystal Sheets of Borophene on Cu(111) Surfaces. *Nat. Nanotechnol.* **2019**, *14*, 44−49.
(42) Ranjan, P.; Sahu, T. K.; Bhushan, R.; Yamijala, S. S.; Late, D. J.; Kumar, P.; Vinu, A. Freestanding Borophene and Its Hybrids. *Adv. Mater.* **2019**, *31*, 1900353.
(43) Mannix, A. J.; Zhou, X.-F.; Kiraly, B.; Wood, J. D.; Alducin, D.; Myers, B. D.; Liu, X.; Fisher, B. L.; Santiago, U.; Guest, J. R.; Yacaman, M. J.; Ponce, A.; Oganov, A. R.; Hersam, M. C.; Guisinger, N. P. Synthesis of Borophenes: Anisotropic, Two-Dimensional Boron Polymorphs. *Science* **2015**, *350*, 1513−1516.
(44) Li, W.; Kong, L.; Chen, C.; Gou, J.; Sheng, S.; Zhang, W.; Li, H.; Chen, L.; Cheng, P.; Wu, K. Experimental Realization of Honeycomb Borophene. *Science Bulletin* **2018**, *63*, 282−286.
(45) Kiraly, B.; Liu, X.; Wang, L.; Zhang, Z.; Mannix, A. J.; Fisher, B. L.; Yakobson, B. I.; Hersam, M. C.; Guisinger, N. P. Borophene Synthesis on Au(111). *ACS Nano* **2019**, *13*, 3816−3822.
(46) Tai, G.; Hu, T.; Zhou, Y.; Wang, X.; Kong, J.; Zeng, T.; You, Y.; Wang, Q. Synthesis of Atomically Thin Boron Films on Copper Foils. *Angew. Chem., Int. Ed. Engl.* **2015**, *54*, 15473−15477.
(47) Wu, R.; Gozar, A.; Božović, I. Large-Area Borophene Sheets on Sacrificial Cu(111) Films Promoted by Recrystallization from Subsurface Boron. *npj Quantum Mater.* **2019**, *4*, 1−6.
(48) Karmodak, N.; Jemmis, E. D. The Role of Holes in Borophenes: An Ab Initio Study of Their Structure and Stability with and without Metal Templates. *Angew. Chem.* **2017**, *129*, 10227−10231.
(49) Karmodak, N.; Jemmis, E. D. Metal Templates and Boron Sources Controlling Borophene Structures: An Ab Initio Study. *J. Phys. Chem. C* **2018**, *122*, 2268−2274.
(50) Ranjan, P.; Lee, J. M.; Kumar, P.; Vinu, A. Borophene: New Sensation in Flatland. *Adv. Mater.* **2020**, *32*, 2000531.
(51) Kaneti, Y. V.; Benu, D. P.; Xu, X.; Yuliarto, B.; Yamauchi, Y.; Golberg, D. Borophene: Two-Dimensional Boron Monolayer: Synthesis, Properties, and Potential Applications. *Chem. Rev.* **2022**, *122*, 1000−1051.
(52) Mazaheri, A.; Javadi, M.; Abdi, Y. Chemical Vapor Deposition of Two-Dimensional Boron Sheets by Thermal Decomposition of Diborane. *ACS Appl. Mater. Interfaces* **2021**, *13*, 8844−8850.
(53) Sheng, S.; Wu, J.-B.; Cong, X.; Zhong, Q.; Li, W.; Hu, W.; Gou, J.; Cheng, P.; Tan, P.-H.; Chen, L.; Wu, K. Raman Spectroscopy of Two-Dimensional Borophene Sheets. *ACS Nano* **2019**, *13*, 4133−4139.
(54) Li, L.; Schultz, J. F.; Mahapatra, S.; Liu, X.; Shaw, C.; Zhang, X.; Hersam, M. C.; Jiang, N. Angstrom-Scale Spectroscopic Visualization of Interfacial Interactions in an Organic/Borophene Vertical Heterostructure. *J. Am. Chem. Soc.* **2021**, *143*, 15624−15634.
(55) Hu, J.; Zhong, C.; Wu, W.; Liu, N.; Liu, Y.; Yang, S. A.; Ouyang, C. 2D Honeycomb Borophene Oxide: A Promising Anode Material Offering Super High Capacity for Li/Na-Ion Batteries. *J. Phys.: Condens. Matter* **2019**, *32*, 065001.
(56) Liao, Q.; Li, N.; Jin, S.; Yang, G.; Wang, C. All-Solid-State Symmetric Supercapacitor Based on Co3O4 Nanoparticles on Vertically Aligned Graphene. *ACS Nano* **2015**, *9*, 5310−5317.
(57) Yang, L.; Cheng, S.; Ding, Y.; Zhu, X.; Wang, Z. L.; Liu, M. Hierarchical Network Architectures of Carbon Fiber Paper Supported Cobalt Oxide Nanonet for High-Capacity Pseudocapacitors. *Nano Lett.* **2012**, *12*, 321−325.
(58) Liu, S.; Kang, L.; Zhang, J.; Jung, E.; Lee, S.; Jun, S. C. Structural Engineering and Surface Modification of MOF-Derived Cobalt-Based Hybrid Nanosheets for Flexible Solid-State Supercapacitors. *Energy Storage Materials* **2020**, *32*, 167−177.
(59) Liu, S.; Kang, L.; Zhang, J.; Jun, S. C.; Yamauchi, Y. Carbonaceous Anode Materials for Non-Aqueous Sodium- and Potassium-Ion Hybrid Capacitors. *ACS Energy Lett.* **2021**, *6*, 4127−4154.

https://doi.org/10.1021/acsmaterialslett.2c00475
ACS Materials Lett. 2022, 4, 1929−1936